



α -Helical peptide vesicles with chiral membranes as enantioselective nanoreactors†

 Xi Chen, Yanqiu Wang, Huaxin Wang, Yongju Kim and Myongsoo Lee *

 Cite this: *Chem. Commun.*, 2017, 53, 10958

 Received 28th July 2017,
Accepted 13th September 2017

DOI: 10.1039/c7cc05869a

rsc.li/chemcomm

We report peptide vesicles with chiral membranes as enantioselective nanoreactors. The peptide vesicles are able to selectively encapsulate only a single enantiomer from a racemic mixture solution through preferential diffusion across the membranes. Notably, the confined space of the vesicle acts as an enantioselective nanoreactor for the encapsulated enantiomer which undergoes further chemical transformations to yield a highly enantiopure product.

In living cells, many biological processes occur within compartments surrounded by a lipid membrane which is selectively permeable to maintain homeostasis by regulating the passage of some substances while preventing others from entering the interior. The membrane encloses catalytically active species in a confined space to protect them from the surrounding environment and allows access and release of chemical substances into and out of the compartments through active and passive diffusions in which chemical transformations take place.¹ Dendrimers and vesicles as biological mimics have been constructed using the self-assembly of amphiphilic molecules with the aim to obtain a confined space.² For example, the dendrimers consisting of hydrophobic, catalytic cores and hydrophilic exteriors can be used to create a confined space for chemical reactions to occur in aqueous solution.^{3–6} Within the confined inner space provided by the dendritic architecture, reactions can proceed with higher selectivity and greatly enhanced reaction rates.

Another example is provided by amphiphilic block copolymer vesicles which have been used to encapsulate many different cargos, especially enzymes to generate catalytic compartments to improve the efficiency and selectivity of the catalytic process.^{7–9} Various amphiphilic block copolymers have been employed to produce vesicles with different sizes and membrane thicknesses to be used as nanoreactors. The membranes consist of a middle hydrophobic layer covered by hydrophilic ones on each side

similar to lipid bilayer membranes. For selective chemical reactions to take place inside nanoreactors, specific reactants should be able to enter the interior of the vesicles by selective diffusion through the membrane. The semi-permeability of the membranes plays a profound role in selective access for substrates to the interior of the vesicles.^{7,9} However, most of the polymer vesicles are based on non-chiral membranes which are far from the membrane cavities with chiral environments.¹⁰

Given that folded helical peptides are intrinsic chiral secondary structures, one of the ideal candidates for the construction of chiral membranes is their self-assembly into an extended membrane structure that allows chiral cavities between the helical strands.^{11–15} For example, the incorporation of oligoether side chains into short hydrophobic peptides induces an α -helical conformation through aggregation into vesicular membranes with a chiral void space.¹⁶ However, the vesicles exhibit low chiral discrimination capabilities that hamper the use of the vesicles as highly efficient enantioselective nanoreactors, most probably due to internal chiral peptide layers buried by achiral polymeric surfaces.

To overcome this limitation, we considered that lateral grafting of hydrophobic aromatic segments as self-assembling units into a hydrophilic α -helical peptide would produce highly efficient enantioselective membranes because of the exposure of the α -helical peptide layers with chiral void spaces to the external environment.¹⁷ The hydrophilic α -peptide surfaces would allow remarkable accessibility of enantiomers to chiral cavities. Here, we report peptide vesicles with enantioselective membranes consisting of a planar nematic-like arrangement of short α -helical peptides at the surfaces. The vesicles are able to encapsulate only a single enantiomer from a racemic mixture solution through selective diffusion across the peptide membrane. The selectively captured enantiomer inside the vesicles undergoes a click reaction to yield a highly enantiopure reaction product in a confined space while preventing the opposite enantiomer from entering the interior (Fig. 1). As a result, the confined space can represent a highly efficient enantioselective nanoreactor for transporting the enantiomer which is separated from the external environment by a peptide membrane.

State Key Lab of Supramolecular Structure and Materials, College of Chemistry, Jilin University, Changchun 130012, China. E-mail: mslee@jlu.edu.cn

† Electronic supplementary information (ESI) available: Experimental details, SEM images, TEM images, and spectral data. See DOI: 10.1039/c7cc05869a

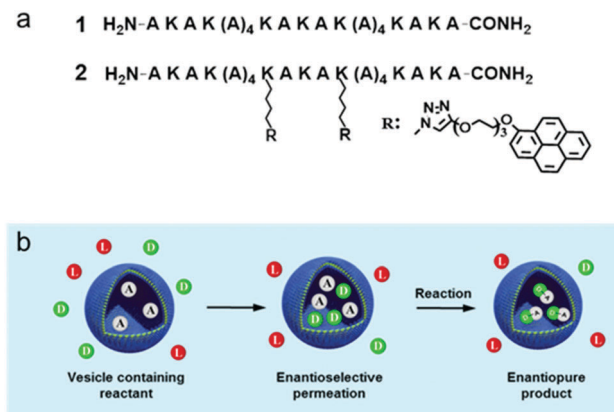


Fig. 1 (a) Chemical structures of **1** and **2**. (b) Schematic representation of a vesicle used as a nanoreactor. Enantioselective permeation and further chemical transformation of D-enantiomers inside the vesicle containing reactant **A**.

The membrane structure of the vesicles consists of a lateral association of rod-like α -helical peptides which allows the vesicular walls to function as a highly efficient enantioselective membrane. The α -helix-forming peptide consists of an AKAK(A)₄KAKAK(A)₄KAKA amino acid sequence with high helix propensity (Fig. 1a).¹⁸ To endow the peptide chain with the self-assembling feature, two pyrenes were symmetrically grafted into the peptide chain through click chemistry of lysine residues with pyrene.¹⁹ The building blocks were synthesized by a solid-state peptide synthesis method with a combination of both natural amino acids and a pyrene-grafted lysine. Peptide **1** with a lack of pyrene adopts a random coil conformation, as confirmed by circular dichroism (CD) measurements, irrespective of concentration changes. However, the incorporation of pyrene into the peptide chains drives the random coil conformation of the peptides to transform into an α -helical one (Fig. 2). The CD spectrum of peptide **2** containing two pyrenes as side groups shows two negative bands at 206 nm and 222 nm, demonstrating that the peptide backbone adopts an α -helical structure.²⁰ Even after adding the helix promoting solvent 2,2,2-trifluoroethanol (TFE), the CD intensity at $\lambda = 222$ nm did not change, indicating nearly maximal helicity.²¹ We envisage that the laterally-grafted rod-like α -helical peptides would be aligned parallel to each other to form flat membranes with a planar nematic-like arrangement.²² Indeed, transmission electron microscopy (TEM) images revealed the formation of spherical objects with diameters ranging from ~ 70 nm to ~ 100 nm (Fig. 2c). Cryo-TEM investigations confirmed the presence of spherical aggregates with a dark outer circle expected from the 2-D projection of hollow vesicles with a uniform thickness of ~ 3 nm (Fig. 2c, inset). Dynamic light scattering (DLS) measurements revealed that the aggregates have an average diameter of ~ 90 nm (Fig. 2b), which is in reasonable agreement with the size observed by TEM. In addition, the concave structures observed in the SEM image indicate the characteristics of deformed hollow spheres formed through the drying process, providing further evidence of the hollow nature of the vesicular structures (Fig. 2d). The results

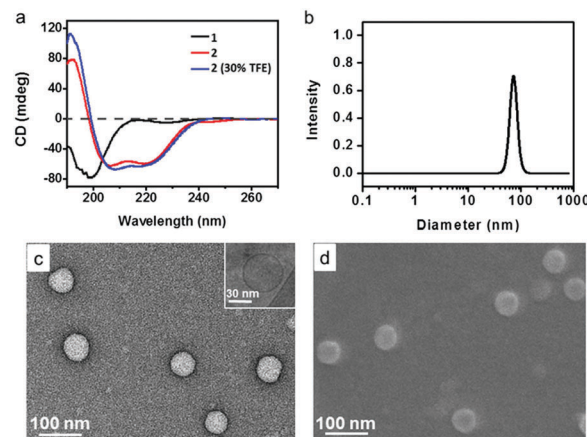


Fig. 2 (a) CD spectra of **1** and **2**, each in 0.1 wt% aqueous solution, (b) DLS traces of **2** in 0.1 wt% aqueous solution. (c) TEM image of **2**; inset, a cryo-TEM image. (d) SEM image of **2**.

demonstrate that the helical conformation triggers the formation of the membrane structures.

To gain insight into the formation of the hollow spherical structure, we performed TEM experiments under highly diluted conditions of peptide **2** (Fig. 3a–c). The images showed the coexistence of ~ 3 nm sized micelles and laterally-associated small fragments of flat membrane structures which begin to deform into buds at 0.003 wt% and then transform into vesicles at 0.1 wt%, most probably due to lowering of the surface energy.²³ Considering the calculated wall thickness and height of the dimer to be ~ 3 nm, the hydrophilic peptide helices are aligned in one-direction, parallel to the flat membrane surface to form peptide bilayers with hydrophobic pyrene units inside (Fig. 3d). The fluorescence emission showed a strong excimer peak in the longer wavelength region together with monomer emission at shorter wavelengths (Fig. S4, ESI[†]), indicative of pyrene packing inside the membranes with packing frustration in the self-assembled state.^{19,24} The results imply that the vesicular structure of peptide **2** originates from budding of the flat membranes consisting of the planar nematic-like

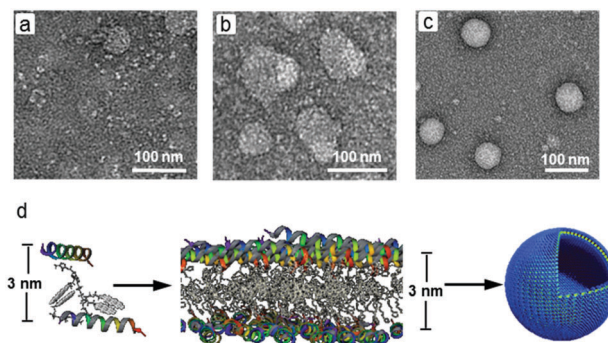


Fig. 3 TEM images of intermediate structures formed at different concentrations of **2**, (a) 0.001 wt%, (b) 0.003 wt%, and (c) 0.1 wt%. (d) Energy-minimized packing structure of the dimeric association of **2** and schematic representation of the self-assembly into a vesicle through flat bilayer membranes as intermediate structures.

alignment of rod-like α -helical peptides on the external surfaces and hydrophobic pyrene inside the membranes (Fig. 3d).

Considering that the vesicular walls consist of planar arrangements of rod-like α -helical peptides on the membrane surfaces with frustrated pyrene packing inside the membranes, the vesicular membranes are intrinsically porous with chiral void spaces between the helical peptide arrangements.^{16,25} Accordingly, we envisioned that the vesicular walls function as enantioselectively permeable membranes.²⁶ To corroborate the permeability of the vesicular walls, we added protected amino acids (0.02 mM) to a solution of peptide 2 at room temperature. The internalization of a series of amino acid derivatives into the vesicular interior was monitored by tracing high-performance liquid chromatography (HPLC) after separation of the free racemate from the solution using a Sephadex column. The concentration measurements of the internalized racemic guests showed that the smaller molecules diffuse into the vesicular interiors faster than the larger molecules (Fig. 4a), indicative of the size-selective permeability of the vesicular walls.

More importantly, the internalization of the guests across the vesicular walls is enantioselective as the diffusion rates of each enantiomer are prominently different (Fig. S5, ESI[†]). The (L)-enantiomers of both mono-peptides, **G1** and **G2**, are internalized faster than the (D)-enantiomers, while their enantioselectivities in enantiometric excess (ee%) decrease over diffusion time (Fig. 4b). The enantioselectivity of **G2** is larger than that of **G1**, indicative of inverse proportionality between permeability and enantioselectivity. Notably, the larger dipeptide, **G3**, is internalized into the vesicle interiors with perfect enantioselectivity with an ee value of 100% up to 4 h permeation, and thereafter gradually

decreases. This result indicates that the peptide vesicles are able to encapsulate only a single enantiomer in racemates above a certain size of the guest through enantioselective diffusion across the vesicular membranes (Fig. 4c). The preferential internalization is attributed to the lateral arrangements of helical peptides parallel to the basal plane which generate chiral porous membrane structures. The chiral void spaces of vesicular membranes would preferentially associate with one enantiomer over the other due to the large difference in free energy required to fit into the voids. Indeed, isothermal titration calorimetry (ITC) measurements with **G2** revealed that the binding affinity for the L-enantiomer is higher ($K_a = 14\,867 \pm 1273$) than that of the D-enantiomer ($K_a = 7503 \pm 160$) (Fig. S6, ESI[†]). This result suggests that the preferential association with membrane voids facilitates selective diffusion across the membrane.

The preferential diffusion led us to envision that the peptide vesicles can be used as enantioselective nanoreactors that provide protected spaces by peptide membranes for the chemical reactions of transporting enantiomers from the environment. To explore the capability of the peptide vesicles as enantioselective nanoreactors, *N*₃-substituted trp-lys dipeptide **G4** was selected to carry out a click reaction with an alkyne-functionalized hydrophilic dendrimer, **A**, because dipeptide **G4** shows perfect enantioselectivity up to 4 h permeation (Fig. 5a), similar to **G3**. It should be noted that the D-form internalizes preferentially to the L-form, as opposed to the other amino acids. To corroborate enantioselective reactions inside the vesicular cavities, first we encapsulated dendritic alkyne **A** that remains inside the vesicles without leakage. The encapsulation of reactant **A** inside the vesicles was confirmed by

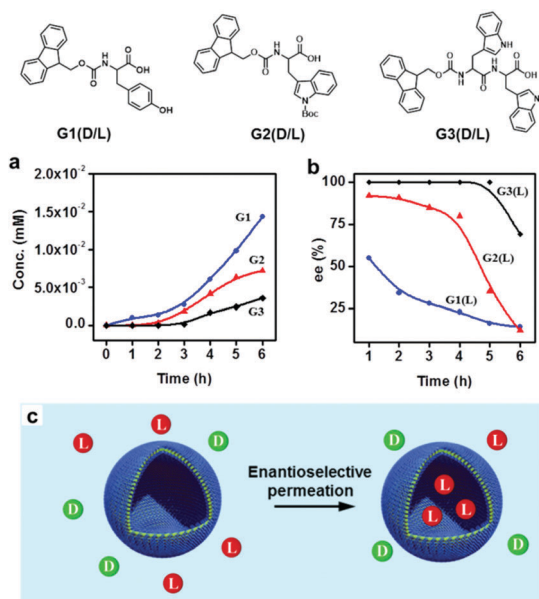


Fig. 4 Molecular structures of racemic amino acids. (a) Permeation of racemic amino acids into the interior of the vesicle with diffusion time. (b) Enantiomeric excess (ee%) of encapsulated L-enantiomers as a function of time. (c) Schematic representation of enantioselective permeation. D; D-enantiomer and L; L-enantiomer.

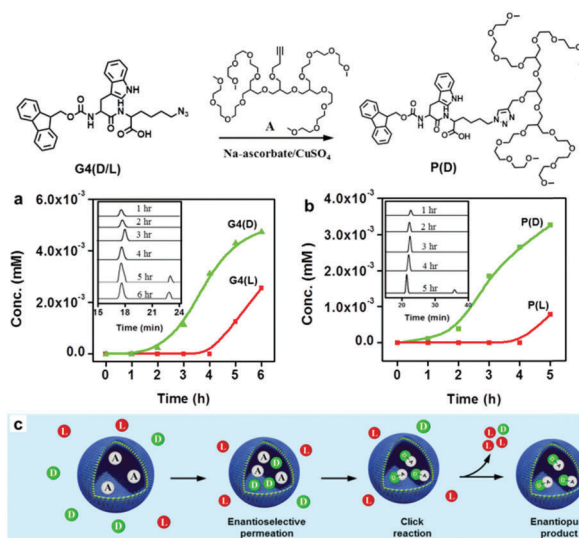


Fig. 5 Click reaction of **G4** and dendritic alkyne **A**. (a) Permeation of each enantiomer of **G4** with diffusion time; inset, HPLC chromatograms of encapsulated enantiomers. (b) Reaction product of each enantiomer formed inside the vesicle with diffusion time; inset, HPLC chromatograms of the reaction products formed from an encapsulated enantiomer. (c) Schematic representation of enantioselective encapsulation and further chemical transformation inside the vesicle nanoreactor. **A**; dendritic alkyne, **D**; D-enantiomer of **G4**, **L**; L-enantiomer of **G4**, **D-A**; reaction product.

MALDI-TOF and HPLC after separation of the untrapped one by gel permeation chromatography (GPC) using a Sephadex LH-20 column. Then, we added racemic **G4** into the vesicle solution encapsulating reactant **A** inside. After 1 h diffusion, MALDI-TOF analysis showed additional peaks corresponding to the reaction product **P** (Fig. S7, ESI[†]), indicating that the click reaction of **G4** readily occurs with the encapsulated dendritic alkyne inside the vesicles (Fig. 5b).

Chiral HPLC analysis showed that the intensity associated with the reaction product of the *D*-enantiomer, **P(D)**, gradually increases without any noticeable traces of the opposite enantiomer product, **P(L)**, over 4 h (Fig. 5b, inset), demonstrating that the vesicular membranes allow only the *D*-enantiomer in the external environment to internalize for click reactions. Because the click reactions between alkyne and azide groups occur rapidly before the other enantiomer (*L*-form) enters into the reaction space, the reaction is able to yield a highly enantiopure product up to 4 h permeation. After 4 h, we found that the *L*-enantiomer begins to undergo a click reaction, leading the enantiopurity of the reaction product to decrease. This result indicates that the interior of the peptide vesicle acts as a highly efficient enantioselective nano-reactor for the entering enantiomer by separating it from the racemic mixture environment (Fig. 5c).

In conclusion, we have demonstrated that a pyrene-substituted helical peptide self-assembles into vesicular structures with enantioselective membranes. The peptide vesicles are able to encapsulate only a single enantiomer from a racemic mixture environment through selective diffusion across the peptide membranes. The encapsulated enantiomer undergoes further chemical reactions inside the vesicles by separating it from the opposite enantiomer in the environment. Such unique vesicles will offer an opportunity to construct versatile reaction spaces for chiral differentiation, facile drug discovery, and enantioselective modifications of intracellular biomolecules.

This work was supported by the 1000 Program and NSFC (no. 51473062, 21574055, 21634005 and 21550110493).

Conflicts of interest

There are no conflicts to declare.

Notes and references

- 1 M. D. Bednarski, H. K. Chenault, E. S. Simon and G. M. Whitesides, *J. Am. Chem. Soc.*, 1987, **109**, 1283.
- 2 K. Renggli, P. Baumann, K. Langowska, O. Onaca, N. Bruns and W. Meier, *Adv. Funct. Mater.*, 2011, **21**, 1241; C. G. Palivan, O. Fischer-Onaca, M. Delcea, F. Itel and W. Meier, *Chem. Soc. Rev.*, 2012, **41**, 2800.
- 3 D. M. Vriezema, M. Comellas Aragonès, J. A. Elemans, J. J. Cornelissen, A. E. Rowan and R. J. Nolte, *Chem. Rev.*, 2005, **105**, 1445.
- 4 D. Astruc, E. Boisselier and C. Ornelas, *Chem. Rev.*, 2010, **110**, 1857.
- 5 G. R. Newkome and C. D. Shreiner, *Polymer*, 2008, **49**, 1.
- 6 M. Kimura, M. Kato, T. Muto, K. Hanabusa and H. Shirai, *Macromolecules*, 2000, **33**, 1117.
- 7 S. F. van Dongen, H. P. M. de Hoog, R. J. Peters, M. Nallani, R. J. Nolte and J. C. van Hest, *Chem. Rev.*, 2009, **109**, 6212.
- 8 D. M. Vriezema, P. M. Garcia, N. Sancho Oltra, N. S. Hatzakis, S. M. Kuiper, R. J. Nolte, A. E. Rowan and J. van Hest, *Angew. Chem., Int. Ed.*, 2007, **46**, 7378.
- 9 S. F. van Dongen, M. Nallani, J. J. Cornelissen, R. J. Nolte and J. van Hest, *Chem. – Eur. J.*, 2009, **15**, 1107.
- 10 Q. Shen, L. Wang, H. Zhou, L. S. Yu and S. Zeng, *Acta Pharmacol. Sin.*, 2013, **34**, 998; A. Mohanty and A. Dey, *J. Chromatogr. A*, 2006, **1128**, 259.
- 11 S. Kimura, D. H. Kim, J. Sugiyama and Y. Imanishi, *Langmuir*, 1999, **15**, 4461.
- 12 E. P. Holowka, V. J. Sun, D. T. Kamei and T. J. Deming, *Nat. Mater.*, 2007, **6**, 52.
- 13 D. W. Lee, T. Kim, I.-S. Park, Z. Huang and M. Lee, *J. Am. Chem. Soc.*, 2012, **134**, 14722.
- 14 Y. B. Lim, K. S. Moon and M. Lee, *Angew. Chem., Int. Ed.*, 2009, **48**, 1601.
- 15 S. Sim, Y. Kim, T. Kim, S. Lim and M. Lee, *J. Am. Chem. Soc.*, 2012, **134**, 20270.
- 16 X. Chen, Y. He, Y. Kim and M. Lee, *J. Am. Chem. Soc.*, 2016, **138**, 5773.
- 17 A. Higuchi, M. Tamai, Y. A. Ko, Y. I. Tagawa, Y. H. Wu, B. D. Freeman, J. T. Bing, Y. Chang and Q. D. Ling, *Polym. Rev.*, 2010, **50**, 113.
- 18 S. Marqusee, V. H. Robbins and R. L. Baldwin, *Proc. Natl. Acad. Sci. U. S. A.*, 1989, **86**, 5286.
- 19 I. Choi, I. S. Park, J. H. Ryu and M. Lee, *Chem. Commun.*, 2012, **48**, 8481.
- 20 D. Aili, K. Enander, J. Rydberg, I. Nesterenko, F. Björefors, L. Baltzer and B. Liedberg, *J. Am. Chem. Soc.*, 2008, **130**, 5780.
- 21 A. D. de Araujo, H. H. Hoang, W. M. Kok, F. Diness, P. Gupta, T. A. Hill, R. W. Driver, D. A. Price, S. Liras and D. P. Fairlie, *Angew. Chem., Int. Ed.*, 2014, **53**, 6965.
- 22 E. Lee, J. K. Kim and M. Lee, *Angew. Chem., Int. Ed.*, 2009, **48**, 3657; D. J. Hong, E. Lee, H. Jeong, J. K. Lee, W. C. Zin, T. D. Nguyen, S. C. Glotzer and M. Lee, *Angew. Chem., Int. Ed.*, 2009, **48**, 1664.
- 23 Y. Kim and M. Lee, *Chem. – Eur. J.*, 2015, **21**, 11836.
- 24 R. Zhang, D. Tang, P. Lu, X. Yang, D. Liao, Y. Zhang, M. Zhang, C. Yu and V. W. Yam, *Org. Lett.*, 2009, **11**, 4302.
- 25 J. Shen and Y. Okamoto, *Chem. Rev.*, 2016, **116**, 1094–1138; C. Li, J. Cho, K. Yamada, D. Hashizume, F. Araoka, H. Takezoe and T. A. Y. Ishida, *Nat. Commun.*, 2015, **6**, 8418.
- 26 R. Xie, L. Y. Chu and J. Deng, *Chem. Soc. Rev.*, 2008, **37**, 1243; K. Shimomura, T. Ikai, S. Kanoh, E. Yashima and K. Maeda, *Nat. Chem.*, 2014, **6**, 429.